Comparison of Shape Memory Effect Between Casting and Forged Alloys of Fe14Mn6Si9Cr5Ni

J.C. Li, M. Zhao, and Q. Jiang

(Submitted 26 November 2001)

The effect of different manufacturing techniques on the shape memory effect (SME) of the Fe14Mn6Si9Cr5Ni alloy has been studied. The SMEs of casting and forged alloys are similar. At ambient temperature, creep and stress-relaxation experiments of the casting alloy show that the casting alloy presents a good creep rupture strength. The manufactured pipe joints of the casting alloys keep jointing under a tensile force of 20 kN and keep sealing under a pressure of 5 MPa. Those excellent mechanical properties satisfy the requirements for pipe jointing in general industrial applications.

Keywords casting alloy, mechanical properties, shape memory alloy, shape memory effect

1. Introduction

Iron-based shape memory alloys have been studied widely due to their low cost and large temperature hysteresis.[1-3] Among the iron-based alloys, FeMnSiCrNi alloys have the best shape memory effect (SME).[4] A theory of the composition design to obtain the best SME has been developed.[5,6] The SME of FeMnSiCrNi alloys is based on a transformation of γ face-centered cubic (fcc) phase to ϵ hexagonal close packed (hcp) phase by the extension and contraction of stacking faults. Thermomechanical training, which increases as the amount of directional ϵ phase increases, is one of the most important measures used to improve the SME of iron-based shape memory alloys.[7,8] The manufactured pipe joint of the Fe14Mn6Si9Cr5Ni-forged alloy keeps sealing up to 5 MPa, which is good enough for the general application of pipe joints. Now, an underground, jointed, oil transport pipeline that is 100 m in length works without a leak for five years.[9,10] However, for actual application, the seamless pipe is too expensive for the standard welding technique used for coupling. The best way to decrease the cost of the pipe joint is to use a casting alloy pipe joint, if its SME is the same as that of the forged alloy. Thus, in this study, the SME of the casting pipe joint was measured and compared with the seamless pipe joint. It has been found that both alloys have almost the same SME, and that the amount of recovery strain and creep resistance are the most important mechanical properties. The former is related to the possibility of sealing and joining pipes, and the latter is related to the working life of the couplings. These properties were measured to confirm that the casting alloys could be utilized in the same way as the seamless pipe.

J.C. Li, M. Zhao, and **Q. Jiang,** Laboratory of Automobile Materials of Ministry of Education and Department of Materials Science and Engineering, Jilin University, Changchun 130025, China. Contact e-mail: jiangq@jlu.edu.cn.

2. Experimental Procedures

The alloys were prepared from Fe, Mn, Si, Cr, and Ni with purities of 98.0, 99.7, 99.0, 99.0, and 99.9%, respectively, and were melted in an induction furnace and cast into ingot. A part of the ingot was forged. Some of the ingots were rolled into plates, and some of them were drawn out pipes. Another part of the ingot was melted again and was cast as pipe joints and plates. The composition of the forged alloy (as determined by chemically analysis) was Fe14Mn6Si9Cr5Ni, where the C content is <0.02%. The casting alloy has almost the same composition of alloying elements but has a double C content of 0.05%. The size of the pipes obtained is ϕ 30 mm in diameter and 3.5 mm for pipe wall thickness. Both the pipes and the plates were solution-treated at 1373 K for 1 h and were quenched into water. The specimens were obtained by cutting the plates using a Mo filament cutter. The sizes of the specimens for the bending experiments and the creep and stress relaxation experiments were 75.0 × 7.0 × 0.5 mm and 100.0 × 3.5 × 1.0 mm, respectively. To obtain a slick internal surface for the pipe joint for coupling with a good sealing property, the pipe joint was processed by turning.

The specimen was bent 180° around a steel rod with a diameter (d) at ambient temperature . The schematic diagram of the bending experiment is shown in Fig. 1. The prestrain ϵ_p was estimated approximately by $\epsilon_p = t/d$ (t is thickness of the specimen) where different values of ϵ_p were obtained through changing d with a constant t. The θ_u (the angle difference before and after the unloading of the stress) was measured to determine the SME. To measure the recovery strain, the bent specimens were annealed at 873 K for 0.5 h. θ_a (the subsequent angle difference before and after annealing) was measured, and the percentage of shape recovery strain (f) in the experiments was determined as follows:

$$f = \theta_u/(180 - \theta_a) \quad \text{(Eq 1)}$$

Experiments of creep under constant stress and stress relaxation under constant strain were performed using a self-built loading device. The testing times used were 3200 and 2600 h, respectively. The constant stress for the creep experiments was

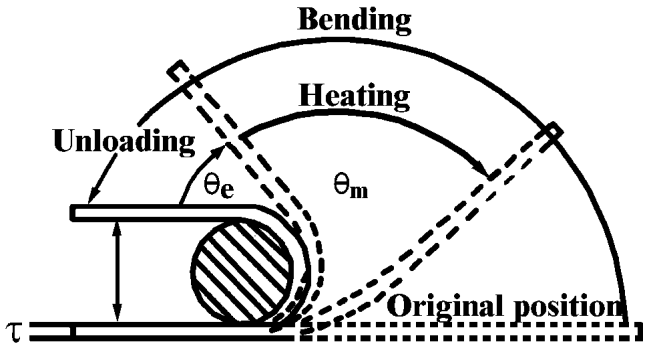

Fig. 1 The schematic diagram for the bending experiment

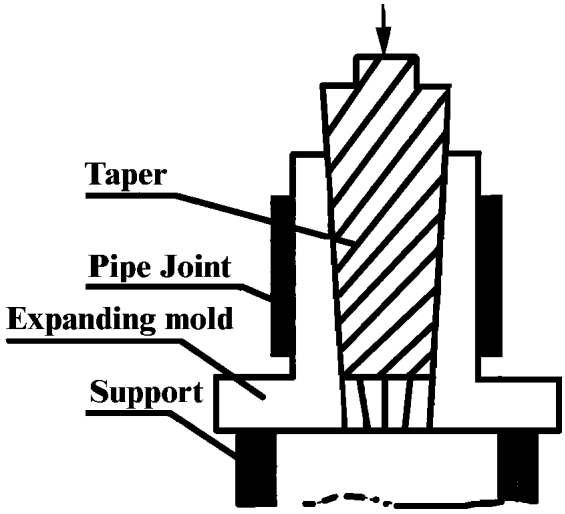

Fig. 2 The schematic diagram for expanding the pipe joint

190 MPa, corresponding to the low-yield stress of the austenite in the range of $\sigma_{0.2} = 180 - 300$ MPa.[1,2] A constant strain of 4% was employed for the stress relaxation measurement. The constant strain corresponds to a stress of 533 MPa to seal and join pipes.

Only the recovery strain in the direction of the radius is favorable to the pipe joint, and homogeneous deformation assures the sealing of the pipe. To assure homogeneous deformation along the direction of the radius, the pipe joint was expanded in the direction of the radius at ambient temperature, the schematic diagram of which is shown in Fig. 2. The absolute recoverable strain, ϵ_a, is calculated as:

$$\epsilon_a = (d_1 - d_2)/d_0, \quad \text{(Eq 2)}$$

where d_0, d_1, and d_2 are the internal diameter of the pipe joint before and after the pipe joint was expanded and after heating at 673 K for 20 min, respectively.

Before any coupling, the pipe joints were first trained, which is in fact the expansion-heating-recovery process described above. This process improves the SME. After the training, two pipes with an external diameter ϕ31.5 mm were joined with the pipe joint at 673 K (Fig. 3). After the jointing parts of the outside of the connecting pipes were turned, the casting pipe joints coupled two pipes. The tensile test for the coupling was made on an Instron machine (Canton, MA). The sealing test for the pipe joining was carried out under hydraulic pressure.

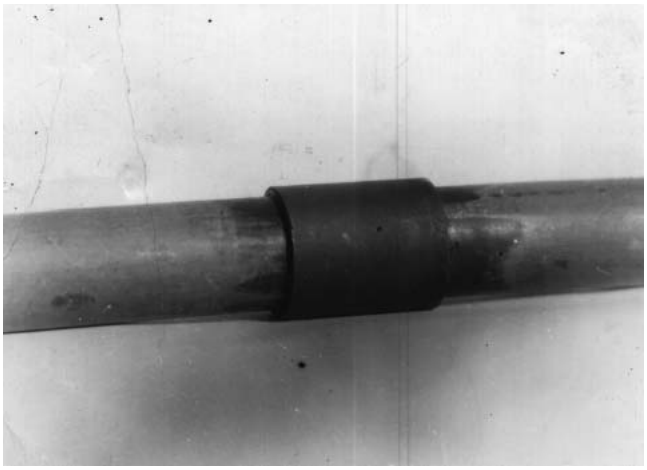

Fig. 3 The pipe joint of the Fe14Mn6Si9Cr5Ni casting alloy

3. Results and Discussion

Figure 4 shows the micrograph of the alloy in which the grain of the casting alloy is dendritic and some carbide is precipitated from austenite phase, which blocks the martensite transition. It is evident that the amount of carbon increases due to the casting process. Thus, a solution treatment is more important for the casting alloy than for the forged alloy. After the solution treatment, the structure of the casting alloy consisted of a single austenitic phase. Now, the structures of the casting alloy and the forged alloy are almost the same, as shown in Fig. 4(b) and (c), although the forged alloy has a greater stacking fault but a smaller grain size than the casting alloy. These differences imply that the forged alloy has lower stacking fault energy within the crystals due to lower C constant[8] and smaller grain size after the forging and before the solution treatment.

The SME of both the casting and forged alloys were measured. f as a function of ϵ_p is shown in Fig. 5. $f(\epsilon_p = 2\%) = 87.5\%$ and $f(\epsilon_p = 5\%) = 57\%$ for the casting alloy, $f(\epsilon_p = 2\%) = 89\%$ and $f(\epsilon_p = 5\%) = 59\%$ for the forged alloy, which are almost the same. The similarity could be induced by the compensation of the grain size and the size of the stacking fault energy, while the casting alloy has a larger grain size and a larger value of stacking fault energy than the forged alloy, as observed in Fig. 4. The larger grain size improves the SME, while the greater value of stacking fault energy deteriorates the SME.[6]

The corresponding strengths and elongations are given in Table 1 where both alloys again present almost the same values. The casting alloy has a slightly higher value for σ_b and slightly lower values for $\sigma_{0.2}$ and δ than the forged alloy. These small distinctions may be induced by the small difference in C content. The increase of C content leads to increased strength, but decreased plasticity.

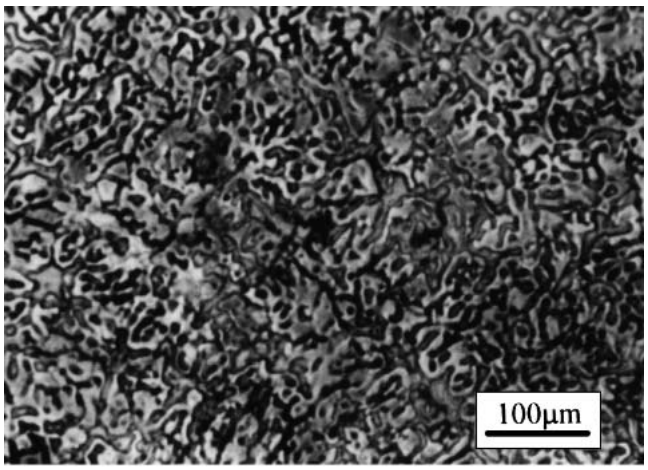

(a)

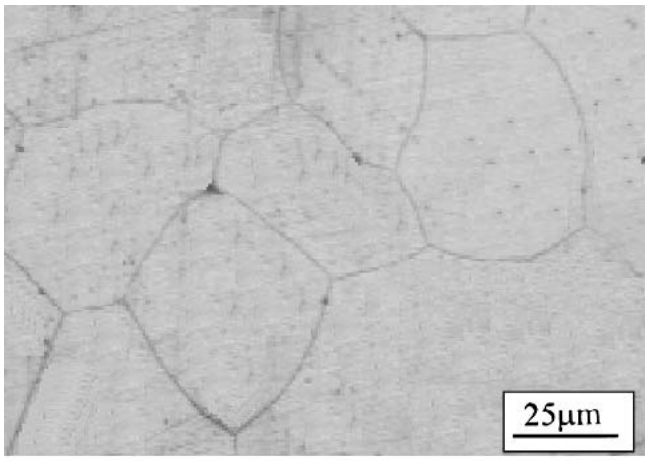

(b)

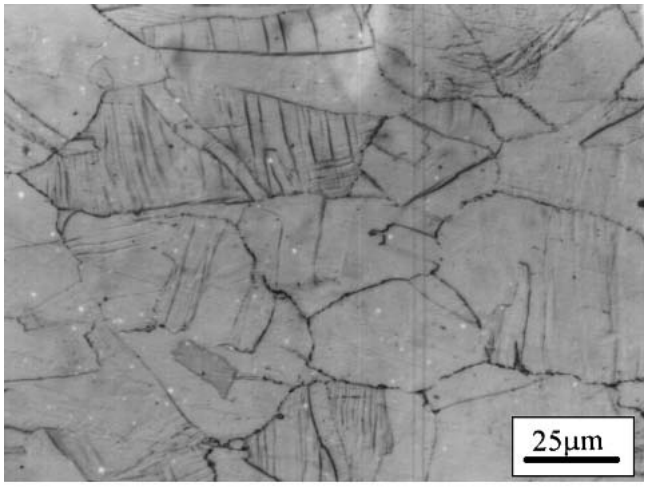

(c)

Fig. 4 Micrograph of the alloys: **(a)** the casting alloy; **(b)** the casting alloy after solution treatment; and **(c)** the forged alloy

The creep and the stress-relaxation experiments of the alloy at ambient temperature are shown in Fig. 6. As the time τ increases, the creep rate decreases. It decreases to 0 as τ becomes >2600 h. The largest amount of creep is 0.2%, which is 3% of the largest absolute recoverable strain (6.2%). The stress relaxation curve shows a similar result. At the beginning, σ decreases quickly. The rate of stress relaxation gradually decreases as τ increases. When τ = 900 h, the stress remains almost constant. The lowest σ at τ >2000 h is 512 MPa, which is about 96% of the original stress. The creep and stress-relaxation properties of the alloy show that the alloy is suitable for application on pipe joints with long working lives.

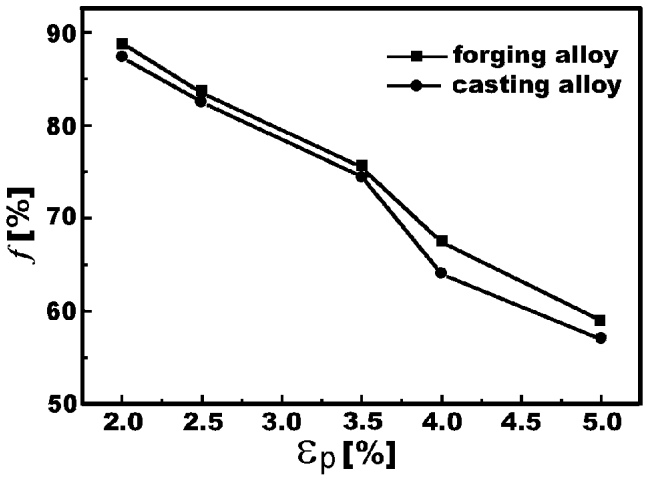

Fig. 5 f for Fe14Mn6Si9Cr5Ni alloys

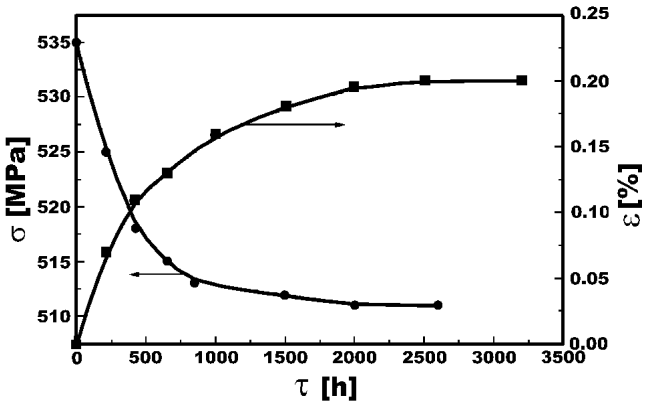

Fig. 6 Creep strain (■) and the stress relaxation (●) of the alloy

Table 1 Tensile Strength of σ_b and $\sigma_{0.2}$ and Elongation Ratio δ of the Alloys

Alloy	σ_b (MPa)	$\sigma_{0.2}$ (MPa)	δ (%)
Casing	863	412	32
Forged	848	419	36

The measured ϵ_a values of the casting and forged alloys are shown in Table 2. Although the ϵ_a of the casting alloy is slightly less than that of the forged alloy, it is large enough for pipe joints (for industrial application, the necessary ϵ_a value is about 3%, which is related to the allowable error of the pipes[10]).

Table 2 Measured Absolute Recoverable Strains of Pipe Joints

Pipe Joint	d_0	d_1	d_2	ϵ_p (%)	ϵ_a (%)
Forged	30.16	31.80	30.84	5.16	3.02
Forged	30.08	31.69	30.68	5.08	3.19
Forged	30.10	31.76	30.79	5.23	3.06
Casting	30.10	31.80	30.59	5.64	2.80
Casting	30.05	31.75	30.87	5.65	2.90
Casting	30.15	31.79	30.93	5.44	2.82

While the tensile test of the pipe joint shows that even if the tensile force reaches 20 kN, the pipe joint continues working, the sealing test indicates that the pipe joint keeps sealing up to 5 MPa. Both values are good enough for a general application of pipe joints. Since the usual internal pressure of an oil or water transport pipe is about 0.2 to 0.4 MPa, the above coupling properties may satisfy the industrial requirements.

Note that the small difference noted above between the casting and forged alloys properties is essentially induced by the C content increase due to the remelting and recasting process. In real engineering practices, this procedure is not necessary, as the pipe joint will be cast directly, and the property difference between the alloys will decrease further, and thus may be neglected.

4. Conclusions

- $\cdot f(\epsilon_p = 2\%) = 87.5\%$ and $f(\epsilon_p = 5\%) = 57\%$ for the Fe14Mn6Si9Cr5Ni casting alloy after solution treatment, which is almost the same of that of the forged alloy.
- At ambient temperature, the largest creep of the Fe14Mn6Si9Cr5Ni casting alloy is 0.2% and the largest stress relaxation is 21 MPa. Therefore, this alloy has good prospects for industrial applications in couplings, while the manufactured pipe joints of the alloy with a tensile force of 20 kN and a sealing pressure of 5 MPa satisfy the usual requirements for pipe joining.

Acknowledgments

The authors are grateful for the support of the Trans-Century Training Program Foundation for the Talents by the Ministry of Education of China and the Department of Science and Technology of Jilin Province of China.

References

1. A. Sato and E. Chishima: "Orientation and Composition Dependences of Shape Memory Effect in Fe-Mn-Si Alloys," *Acta Metall.*, 1984, *32*, pp. 539-47.
2. H. Inagaki: "Shape Memory Effect of Fe-14%Mn-6%Si-9%Cr-6%Ni Alloy Polycrystals," *Z. Metallkd.*, 1992, *83*, pp. 90-96.
3. J.H. Yang and H. Chen: "Development of Fe-Based Shape Memory Alloys Associated With Face-Centered-Cubic-Hexagonal Close-Packed Martensitic Transformation: Part I. Shape Behavior; Part II. Transformation; Part III Microstructures," *Metall. Trans. A*, 1992, *23*, pp. 1431-44.
4. Y. Hoshino and N. Nakamura: "In-Situ Observation of Partial Dislocation Motion During $\gamma \rightarrow \epsilon$ Transformation in a Fe-Mn-Si Shape Memory Alloy," *Mater. Trans. JIM*, 1992, *33*, pp. 253-62.
5. J.C. Li, W. Zheng, and Q. Jiang: "Stacking Fault Energy of Iron-Base Shape Memory Alloys," *Mater. Lett.*, 1999, *38*, pp. 275-77.
6. J.C. Li, M. Zhao, and Q. Jiang: "Alloy Design of FeMnSiCrNi Shape Memory Alloys Related to Stacking Fault Energy," *Metall. Mater. Trans. A*, 2000, *30*, pp. 581-84.
7. K. Tsuzaki and M. Ikegami: "Effect of Thermal Cycling on the Martensitic Transformation in a Fe-24Mn-6Si Shape Memory Alloy," *Mater. Trans. JIM*, 1992, *33*, pp. 263-70.
8. L. Federzoni and Q. Gu: "Influence of the Presence of Pre-existing Thermal ϵ-Martensite on the Formation of Stress-Induced ϵ-Martensite and on the Shape Memory Effect of a Fe-Mn-Si-Ni Shape Memory Alloy," *Scripta Metall. Mater.*, 1994, *31*, pp. 25-30.
9. J.C. Li, Z. Zhang, and Q. Jiang: "Properties and Application of Fe-6Si-14Mn-9Cr-5Ni Shape Memory Alloys," *Mater. Sci. Tech.*, 2001, *17*, pp. 292-95.
10. J.C. Li, X.X. Lu, and Q. Jiang: "Effects of Shape Memory Effect in Fe14Mn6Si9Cr5Ni Alloy on Joining Pipe," *ISIJ Int.*, 2000, *40*, pp. 1124-26.